Desalination and Water Treatment
www.deswater.com
doi: 10.5004/dwt.2019.23458

142 (2019) 125–135
February

Research on a coupling model for groundwater depth forecasting

Chao Song[a], Xianqi Zhang[a,b,*], Dengkui Hu[a], Wei Tuo[a]

[a]*College of Water Resources, North China University of Water Resources and Electric Power, Zhengzhou 450046, China. Tel. +86-158-3719-7937; email: 80324427@qq.com (X. Zhang), Tel. +86-131-6436-2272; email: 862967850@qq.com (C. Song), Tel. +86-159-0399-0321; email: 812393140@qq.com (D. Hu), Tel. +86-181-1319-1995; email:1181309403@qq.com (W. Tuo)*
[b]*Collaborative Innovation Center of Water Resources Efficient Utilization and Protection Engineering, Zhengzhou 450046, China*

Received 13 June 2018; Accepted 12 November 2018

ABSTRACT

Groundwater depth forecasting plays an important role in agricultural irrigation, rational utilization of soil and water resources and ecological protection. The groundwater resource system is influenced by multiple factors such as temperature, precipitation, evapotranspiration, surface water recharge and groundwater discharge, it is characterized by randomness and non-stationary. The empirical mode decomposition (EMD) can decompose the signal into sub-signals of different frequencies and can reduce the non-stationary of the original signal, the Elman neural network (ENN) has strong nonlinear approximation ability. Based on the characteristics of the above two methods, the EMD-Elman coupling forecasting model was constructed and applied to groundwater depth forecasting in People's Victory Canal Irrigation District. The results show that EMD-Elman model has better forecasting effect and lower forecasting error and is better than single back propagation neural network model and ENN model. Furthermore, under human over-exploitation, the forecasting accuracy of the EMD-Elman model will be slightly reduced, but the forecasting effect is still in the acceptable range. This research has an important guiding value on revealing People's Victory Canal Irrigation District of groundwater dynamic change rule and provide a new way for groundwater depth forecasting.

Keywords: EMD; ENN; Groundwater depth; Forecasting; People's victory canal irrigation district

1. Introduction

The accurate forecasting of groundwater depth provides an important theoretical foundation for the rational allocation of groundwater in the future irrigated areas. The variation of groundwater depth is a complex hydrological process, there are many factors influence groundwater depth variation such as groundwater pumping, rainfall and topographic conditions [1]. Foreign scholars have done a lot of research on the complex series of groundwater depth and have achieved some fruitful results. Zhang et al. [2] used grey self-memory model, radial basis function neural network and adaptive neuro fuzzy inference system model to forecast groundwater depth of unconfined aquifers in Jilin city. Choi et al. [3] used period-dividing algorithm and response surface methodology to forecast and estimate groundwater levels in Sangchun watershed in Eastern South Korea. Mohanty et al. [4] used artificial neural network to forecast weekly groundwater levels at multiple sites. Mahallawi et al. [5] used generalized regression neural network and linear network to forecast groundwater nitrate pollution in rural areas. Maiti and Tiwari [6] used three kinds of neural networks to forecast underground water level in Dindigul, India. Scholars in China also realized substantial accomplishment in groundwater depth forecasting methodology. Yu et al. [7] used hybrid-wavelet artificial intelligence models to forecast monthly groundwater depth in extreme arid regions, Northwest China. Yang et al. [8] used time series model to predict the dynamic variation of groundwater in Jilin province. Sheng et al. [9] used gray memory model to

* Corresponding author.

forecast the groundwater depth in Xinjiang. Li et al. [10] used a self-memory model to forecast groundwater depth in Shanxi Jinzhong.

As the variation of groundwater depth is not within a fixed movement cycle and presents the characteristics of multiple time scales and local fluctuations, how to deal with the non-linear and non-stationary groundwater depth data becomes the key to forecasting of groundwater depth. Elman neural network (ENN) has a strong independent learning adaptability and generalization ability. It is widely used in the nonlinear time series forecasting model [11]. Empirical mode decomposition (EMD) [12] can separate the low frequency and high frequency part of the signal, thus reducing the non-stationarity of the sequence. Based on the above two methods, the paper mainly forecast the intrinsic modal function (IMF) components of groundwater depth and also analyze whether the forecasting error of IMF components would influence the forecasting error of groundwater depth.

To the best of our knowledge, although the neural network has been applied in forecasting of groundwater depth [13,14]. However, it is rare to combine EMD method and ENN to build a coupling forecasting model of groundwater depth, especially the establishment of different frequency sub-signal forecasting model of groundwater depth is rare. Based on this, the EMD-Elman coupling forecasting model was constructed and applied to groundwater depth forecasting in People's Victory Canal Irrigation District. Furthermore, the paper also discusses whether the forecasting accuracy of these model changes under human over-exploitation. This study is of great significance to guide the scientific management of agricultural water in irrigation district.

2. Research method

2.1. The theory of EMD

EMD was first proposed by Huang et al. [12], it is powerful and adaptive in analyzing the complex nonlinear signal. The signal of EMD is composed of IMFs and residual [15].

In essence, the EMD method is to decompose the nonlinear and non-stationary signals step by step so as to obtain some IMF components and residual of different frequency domain information, so that the decomposed IMF components have obvious physical background.

By applying EMD decomposition to the groundwater depth series, the non-stationarity and volatility of the sequence are reduced and form a series of time series with little mutual impact. This provides a stable series for the forecasting of ENN. Thus, the complex groundwater depth forecasting can be transformed into the sum of forecasting value of several IMF components and residual, the forecasting error of groundwater depth series is determined by these IMF components and residual.

An IMF resulting from the EMD decomposition should satisfy two conditions: (1) in the whole data series, the number of extreme points and the number of zeros must be the same or no more than one; (2) at any time, the envelope mean defined by the signal of local maximum and minimum is zero.

When apply the EMD algorithm to a given groundwater depth series $x(t)$, the procedure to extract the IMF component are shown below:

- Find out the extreme points of the groundwater depth series $x(t)$.
- Use cubic spline curve to connect all the local maximum and minimum points to form upper envelope ($S_{up}(t)$) and lower envelope ($S_{low}(t)$) and calculate the mean value of $S_{up}(t)$ and $S_{low}(t)$.

$$m(t) = \frac{S_{up}(t) + S_{low}(t)}{2} \tag{1}$$

- Assume $h(t)$ is the difference between the groundwater depth sequence $x(t)$ and $m(t)$,

$$h(t) = x(t) - m(t) \tag{2}$$

- Verify whether $h(t)$ meets the definition of IMF components [16], if do not, repeat the steps (1)–(3), until $h_i(t)$is an IMF component and define this IMF component as IMF(t).
- Repeat steps (1)—(4) to get the n IMF components and the corresponding residual.

$$r(t) = x(t) - \mathrm{IMF}_i(t) \tag{3}$$

where $\mathrm{imf}_i(t)$ is newly acquired IMF component.

- Stop the sifting process until the residue function becomes a monotonic function where no more IMF can be extracted [17].

The relationship between the IMF components and the original signal can be represented as follows:

$$x(t) = \sum_{i=1}^{m} \mathrm{IMF}_i(t) + r(t) \tag{4}$$

2.2. Elman neural network

The ENN was proposed by Elman [18]. It is a feedback neural network composed of four layers, which are input layer, hidden layer, receiver layer and output layer respectively, as shown in Fig. 1. There are adjustable weights connecting each two neighboring layers. Generally, it is considered as a special kind of feed-forward neural network with additional memory neurons and local feedback [19]. Compared with back propagation neural network (BPNN), the Elman network adds one layer in the hidden layer as the delay operator to implement the system memory, it makes the system has the ability to adapt to the time-varying and widely used in various fields [20–24]. The Elman network structure is shown in Fig. 1.

The input vector $u(k–1)$ is r-dimensional vector and $u(k–1) = [u_1(k–1), u_2(k–1), \ldots, u_r(k–1)]^T$, the output vector y is the m-dimensional vector and $y(k) = [y_1(k), y_2(k), \ldots, y_m(k)]^T$, x_c is n-dimensional feedback state vector, $w^3(k)$ is the connection

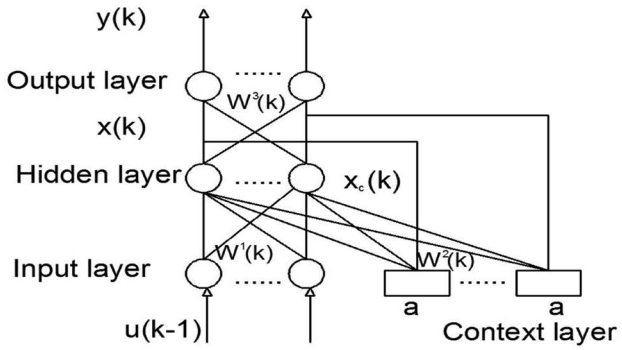

Fig. 1. ENN architecture.

weight of the hidden layer to the output layer, $w^2(k)$ is the connection weight of the input layer to the hidden layer and $w^1(k)$ is the connection weight of the hidden layer to the context layer. The ENN mathematical model is shown in the following Eqs. (5)–(7).

$$y(k) = g(w_2 x(k)) \tag{5}$$

$$x(k) = f(w_2 x_c(k) + w_2(u(k-1))) \tag{6}$$

$$x_c(k) = x(k-1) + a x_c(k-1) \tag{7}$$

where $g()$ is the activation function of the output neuron. It is a linear combination of hidden layers. $f()$ is the activation function of the hidden layer neurons, which is commonly defined as $f(x) = 1/(1 + e^{-x})$. a is the self-connected feedback gain factor and $0 \le a \le 1$. The ENN adopts BPNN algorithm to carry out weight correction, the error of network is as follows:

$$E(w) = \sum_{k=1}^{n} (y_k(w) - \hat{y}_k(w))^2 \tag{8}$$

where $\hat{y}_k(w)$ is the target output vector and $y_k(w)$ is the output vector of object.

2.3. The coupling model of EMD-Elman

The procedure of the EMD-Elman coupling model are as follows:

- Use EMD method to decompose groundwater depth data into several IMF components and one residual.
- Standardize the IMF components and one residual.

If the input data ranges have large difference, the network may exist big forecasting error, so the raw groundwater depth data must standardized and keep it in the range of [0,1], the normalized formula is defined as follows:

$$y = \frac{x - x_{\min}}{x_{\max} - x_{\min}} \tag{9}$$

where x represents original value. $x_{\max}$ and $x_{\min}$ represent the maximum value and minimum value of original data.

- Use the ENN to forecast the IMF components and the residual.
- Add up the forecasting value of IMF components and residual and convert it into the forecasting value of groundwater depth.
- Compare with the original value and calculate the relative error.

$$\delta = \frac{|a-b|}{a} \times 100\% \tag{10}$$

where a represents the original value and b represents forecasting value.

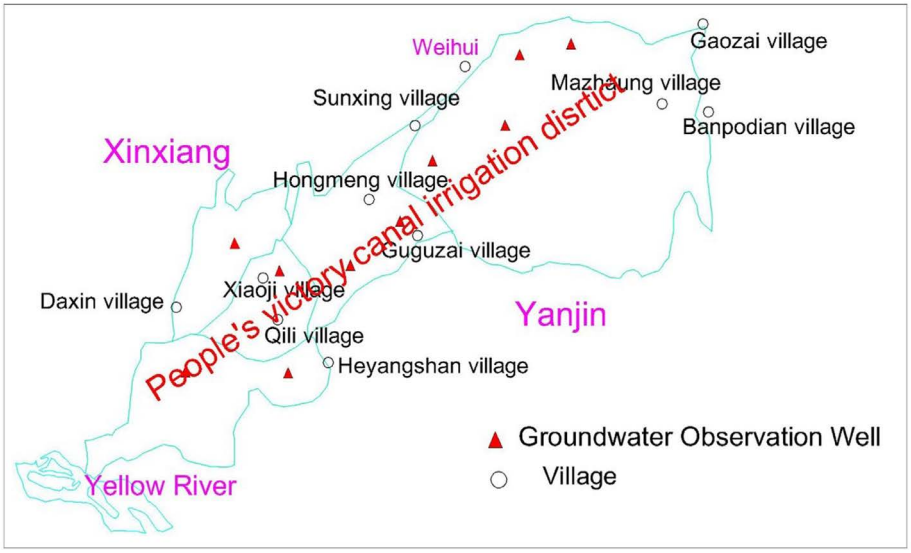

Fig. 2. The location of irrigation district and observation well.

3. Case study

3.1. Study area and data sources

3.1.1. Study area

The People's Victory Canal Irrigation District is located in North Henan province, it is the first large-scale irrigation district in the Yellow River since the foundation of new china. The total control area of the irrigation district is 1,486.84 km^2, mainly irrigating Xinxiang, Anyang, Jiaozuo region (Fig. 2).

3.1.2. Data sources

The data used in this paper come from the measured data in the observation Wells of People's Victory Canal Irrigation District from 1993–2013, the observation Wells data came from the People's Victory Canal Irrigation District administration in Henan province.

As can be seen from Fig. 3, the groundwater depth in the People's Victory Canal Irrigation District showed a rising trend in 1993–2013, which with certain volatility, and the volatility is inconsistent, it also proves that the groundwater depth is uncertain and unstable, this also reflects from the side that it is reasonable to choose the EMD method.

3.2. The EMD decomposition

According to the procedure of EMD decomposition, the decomposition result of groundwater depth is shown in Fig. 4.

As can be seen from Fig. 4, the groundwater depth series is decomposed into five IMF components and one corresponding residual. The first IMF component has the greatest volatility, with the highest frequency and shortest

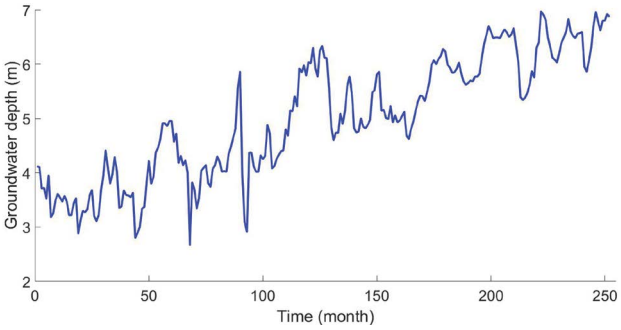

Fig. 3. The groundwater depth curve of the People's Victory Canal Irrigation District from 1993 to 2013.

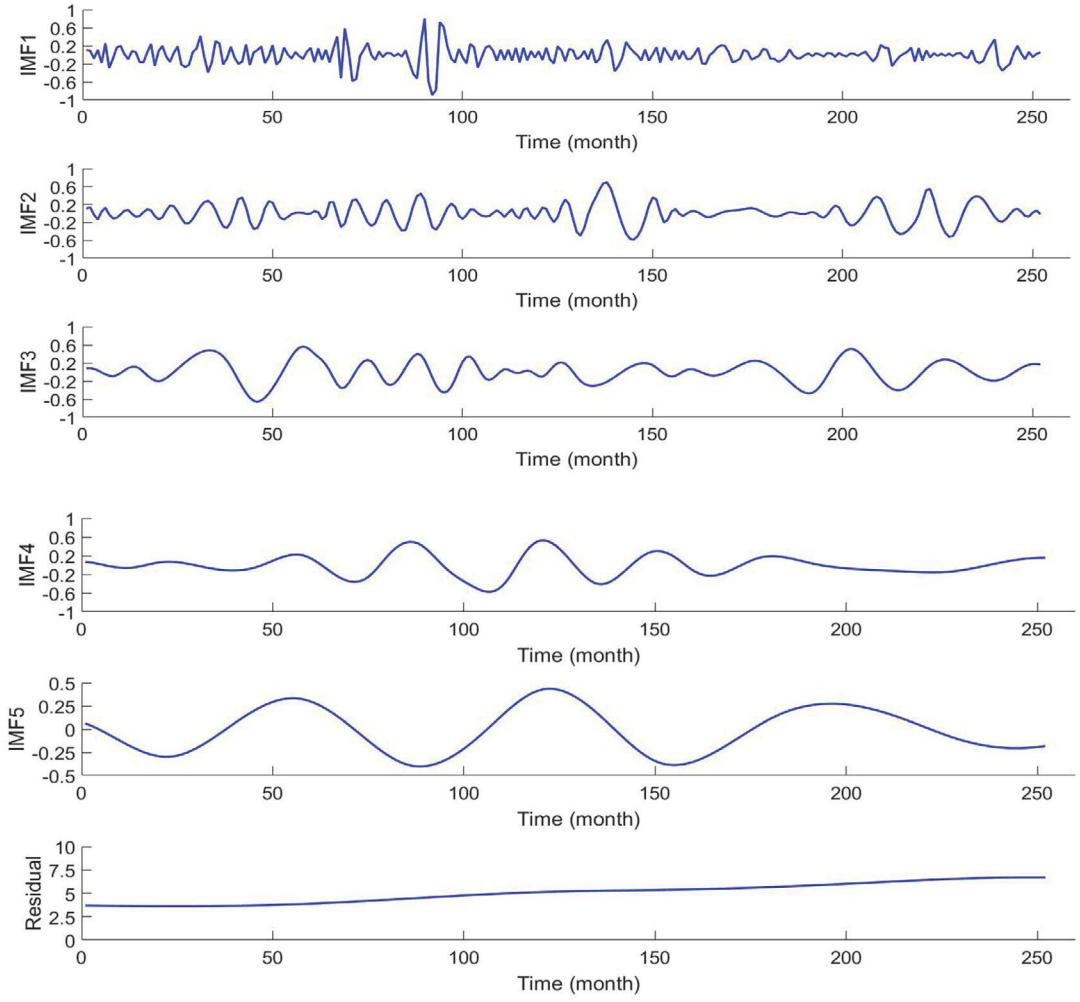

Fig. 4. The result of EMD decomposition.

wavelength. But for other IMF components, the amplitude gradually decreases and the frequency decreases. This shows that after EMD decomposition, the fluctuation and non-stationary of sequence are greatly reduced. Furthermore, EMD decomposition itself is to decompose a series of signals into sub-signals of different frequencies, on this basis, to analyze the contribution of sub-signals of different frequencies to the signal. It can be understood that whether the forecasting error of a certain IMF component will influence the forecasting error of the groundwater depth sequence.

3.3. The construction of coupling model

Take the IMF components and residual data from the 1993–2011 years as the train sample, the IMF components and residual data of the 2012–2013 years as the test sample. The paper adopts the method of rolling prediction, which use the *i*th month in nineteen consecutive years' data to forecast the *i*th month of the twenty year's data.

The related parameters of ENN are set as follows:

Through a large number of repeated tests, the number of hidden layer nodes is determined as 10, the hidden layer neuron transfer function is tansig, the output layer neuron transfer function is purelin, the network training function is the traingdx, the iteration number is 1,000, the accuracy of the network is 10^{-2}. The forecasting effect of IMF components and residual are as shown in Fig. 5.

As can be seen from Fig. 5, the forecasting effect of IMF1 component is slightly poor, this is because IMF1 component is relatively low in stationarity. However, the forecasting

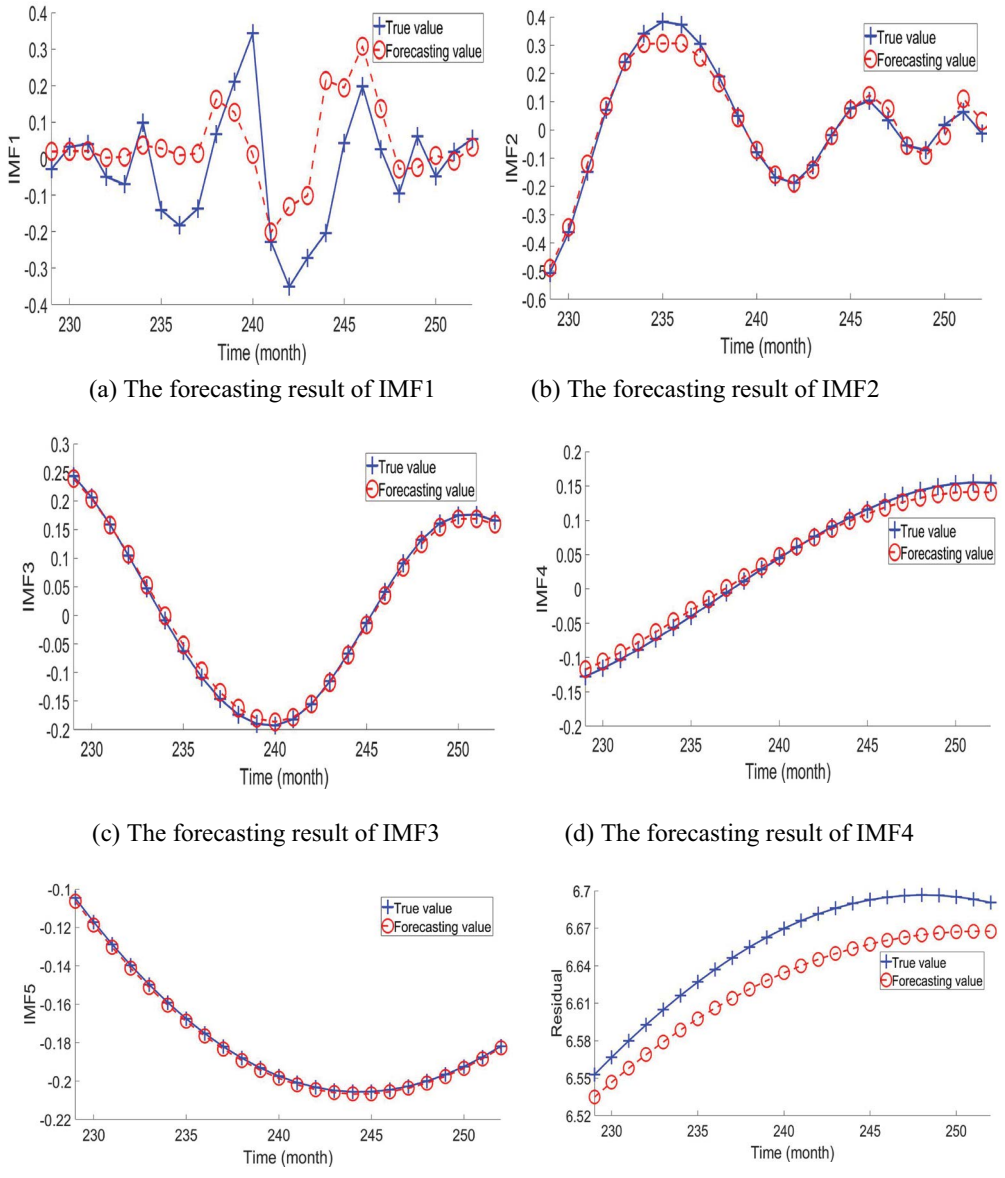

(a) The forecasting result of IMF1

(b) The forecasting result of IMF2

(c) The forecasting result of IMF3

(d) The forecasting result of IMF4

(e) The forecasting result of IMF5

(f) The forecasting result of residual

Fig. 5. The prediction result of IMF1~residual.

effect of IMF2–residual is getting better and better, this indirectly indicates that, after EMD decomposition, the fluctuation and non-stationary of groundwater depth series decrease gradually. Furthermore, as can be seen from the abscissa of Fig. 5, residual accounts for a large proportion, its forecasting error will influence the forecasting error of groundwater depth. IMF1 component is relatively low in stationarity, its forecasting error is relatively large, but it will not have a great impact on the overall forecast error due to its small proportion.

As can be seen from Table 1, the maximum, minimum and mean value of the forecasting relative error of IMF1 component are maximum, the values are 435.58%, 11.42% and 118.14%, respectively. This is because the IMF1 component has relatively low stationarity, leading to a large forecasting error. On the contrary, the maximum, minimum and mean value of the relative error of residual is minimum. The values are 0.54%, 0.27% and 0.45%, respectively. This is because the residual has relatively high stationarity, leading to a small forecasting error.

As can be seen from Table 2, the maximum, minimum and average relative errors are 5.87%, 0.02% and 1.47%, respectively, the forecasting relative error of EMD-Elman model is small and the forecasting accuracy is high.

As can be seen from Fig. 6, the forecasting value of groundwater depth in the People's Victory Canal Irrigation

Table 1
The forecasting relative error of IMF1 ~ residual

IMF	The maximum value of the forecasting relative error (%)	The minimum value of the forecasting relative error (%)	The mean value of the forecasting relative error (%)
IMF1	435.58	11.42	118.14
IMF2	350.83	0.36	41.83
IMF3	91.36	0.25	9.98
IMF4	124.53	1.23	16.32
IMF5	1.49	0.46	0.71
Residual	0.54	0.27	0.45

Table 2
The forecasting error of groundwater depth in people's victory irrigation district from 2012 to 2013

Year	Month	True value (*m*)	Forecasting value (*m*)	Absolute error	Relative error of forecasting (%)
2012	1	6.03	6.08	0.05	0.84
	2	6.21	6.2	–0.01	0.14
	3	6.4	6.39	–0.01	0.08
	4	6.49	6.54	0.05	0.8
	5	6.6	6.66	0.06	0.95
	6	6.83	6.72	–0.11	1.59
	7	6.6	6.68	0.08	1.21
	8	6.52	6.63	0.11	1.74
	9	6.48	6.57	0.09	1.37
	10	6.56	6.61	0.05	0.83
	11	6.57	6.46	–0.11	1.74
	12	6.59	6.24	–0.35	5.37
2013	1	5.96	5.96	0	0.02
	2	5.86	6.04	0.18	3.08
	3	6.06	6.17	0.11	1.85
	4	6.3	6.67	0.37	5.87
	5	6.71	6.81	0.1	1.47
	6	6.96	7.04	0.08	1.14
	7	6.78	6.88	0.1	1.48
	8	6.62	6.64	0.02	0.27
	9	6.8	6.65	–0.15	2.28
	10	6.8	6.77	–0.03	0.45
	11	6.92	6.89	–0.03	0.38
	12	6.87	6.85	–0.02	0.31

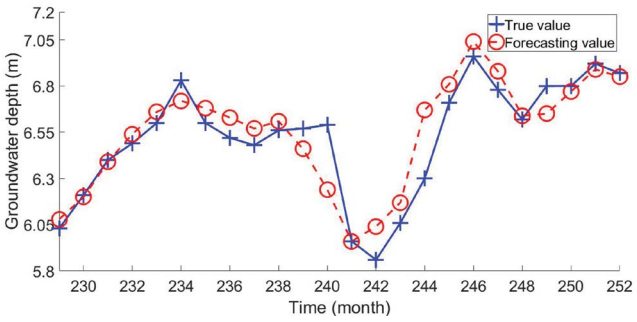

Fig. 6. The forecasting result of value of groundwater depth in people's victory irrigation district from 2012 to 2013.

District from 2012 to 2013 is basically consistent with the true value, and the fitting degree of the model is relatively high.

There are many factors involved in the variation of groundwater depth, and the influencing factors are different each year. Therefore, the paper analyzes the seasonal variation of groundwater depth.

Groundwater depth in spring and summer tends to rise, the reasons can be explained below: in spring, wheat needs more water for irrigation. During the growing stage of wheat, there are three stages that require irrigation, they are sowing–jointing, jointing–heading, and heading–ripening, during this period, the irrigation water demand is larger. Furthermore, when wheat leaves turn green, irrigation water needs to increase. However, to the best of our knowledge, there is less rain in Henan province in January to June, this leads to poor runoff recharge conditions, the villager people have to pump a lot of groundwater for irrigation, so the groundwater depth in April–June showed an increasing trend.

Groundwater depth in autumn tends to decrease. In my opinion, on the one hand, after summer, with the increase of rainfall in summer and the decrease of human exploitation, the groundwater is replenished and the groundwater level begins to rise. In July and August, there was a large amount of precipitation, and crops requiring irrigation were dependent on rainfall and canal irrigation. Some crops were mature and did not need irrigation. On the other hand, the rainfall infiltration replenishment during flood season is higher than that during non-flood season, this also lead to a downward trend in groundwater depth from July to August and an upward trend from January to June.

The groundwater depth in November and January tends to decrease, this is due to more snow and less evaporation consumption, as well as the freezing of soil, resulting in a decrease in groundwater depth.

3.4. Comparison with other models

To compare the forecasting effect of the EMD-Elman coupling model with other single neural network models, the forecasting errors of the three models were made, as shown in Table 3.

As can be seen from Table 3, the EMD-Elman model has a higher qualified rate and a lower relative error and is superior to single BPNN and ENN model, furthermore, the forecasting effect of EMD-Elman model is relatively stable compared with BPNN and ENN model. This shows that EMD-Elman coupling model is feasible for groundwater depth forecasting.

4. Discussion

The variation of groundwater depth mainly depends on precipitation, temperature, human exploitation, topography and landform, geological structure, etc. The most influencing factors are precipitation and artificial exploitation. Precipitation, as the main source of groundwater recharge,

Table 3
Forecasting error of other models

Year	Month	The relative error of EMD-Elman coupling model (%)	The relative error of ENN model (%)	The relative error of BPNN model (%)	Year	Month	The relative error of EMD-Elman coupling model (%)	The relative error of ENN model (%)	The relative error of BPNN model (%)
2012	1	0.84	1.95	2.56	2013	1	0.02	4.33	2.23
	2	0.14	2.98	12.65		2	3.08	6.29	13.3
	3	0.08	7.19	4.32		3	1.85	0.72	0.86
	4	0.80	8.61	14.80		4	5.87	4.22	3.43
	5	0.95	9.49	7.97		5	1.47	11.54	8.76
	6	1.59	11.53	8.01		6	1.14	15.52	10.6
	7	1.21	6.85	12.19		7	1.48	11.23	8.86
	8	1.74	4.00	2.78		8	0.27	6.33	5.89
	9	1.37	3.24	5.31		9	2.28	7.18	6.68
	10	0.83	3.99	15.44		10	0.45	6.06	14.25
	11	1.74	4.50	8.25		11	0.38	7.29	6.73
	12	5.37	5.46	2.33		12	0.31	7.32	6.57

The qualified rate of EMD-Elman coupling model 100%.
The qualified rate of Elman model 83.77%
The qualified rate of BPNN model 70.83%

greatly influences groundwater depth, especially shallow groundwater. But human exploitation is the main way of groundwater consumption. So in the case of serious human over-exploitation, whether the forecasting accuracy of the EMD-Elman model will change, the model analyses the condition of human over-exploitation again.

Suppose the serious over-exploitation occurred in April–June of 2012–2013, Therefore, compared with normal condition, the groundwater depth in April–June is bound to increase, it is assumed that groundwater depth increases by 1 m.

To make the analytical process clearer and easier to understand, the IMF components in the two cases were made, as shown in Fig. 7.

As can be seen from Fig. 7, compared with normal condition, the IMF components under human over-exploitation has significant fluctuations and changes. For IMF5 and residual, the difference value between the two cases is about 0.6; For IMF1–IMF4, it occupies a small proportion in the groundwater depth series, the difference value between the two cases is less.

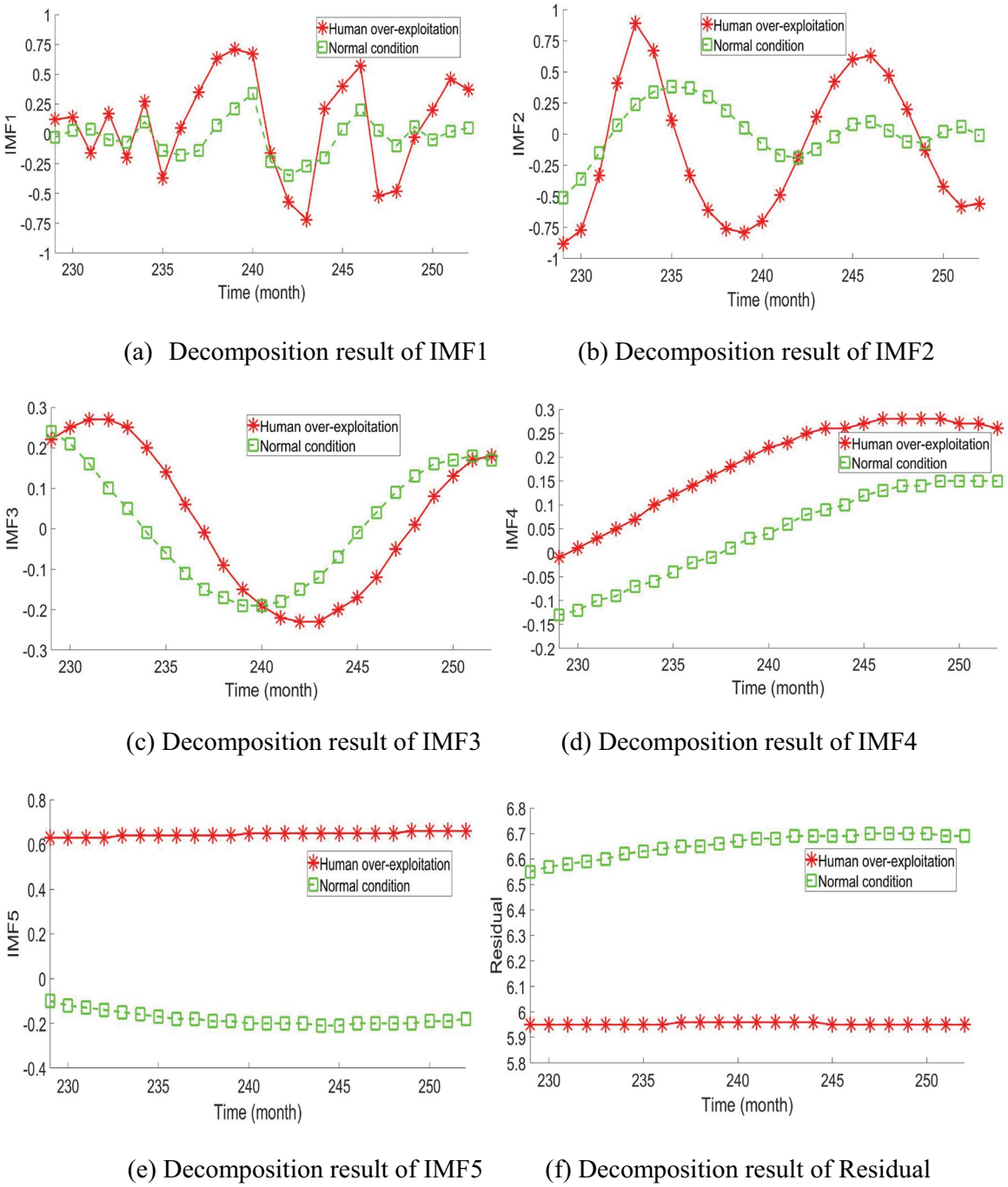

(a) Decomposition result of IMF1

(b) Decomposition result of IMF2

(c) Decomposition result of IMF3

(d) Decomposition result of IMF4

(e) Decomposition result of IMF5

(f) Decomposition result of Residual

Fig. 7. The IMF components and residual in two cases.

In order to verify whether the forecasting accuracy of EMD-Elman model will change under human over-exploitation, the forecasting effect of IMF components and residual were made again as shown in Fig. 8.

As can be seen from Fig. 8, under human over-exploitation, the forecasting effect of IMF1 is poor. For the IMF2–residual, the forecasting effect of the EMD-Elman model is well, this is because IMF2–residual is becoming more and more stable. Furthermore, even under human over-exploitation, EMD can still decompose the complex groundwater depth series into the IMF1 component with a small proportion and the residual with a large proportion. IMF1 component is relatively low in stationarity, the residual is relatively high in stationarity, this explains that in Figs. 5 and 8, the forecasting effect of IMF1 is poor and the forecasting effect of residual is great, but the forecasting error of IMF1 does not influence the forecasting effect of groundwater depth.

In order to reflect the change of the relative error of the model under human over-exploitation and normal condition more intuitively, Table 4 was made.

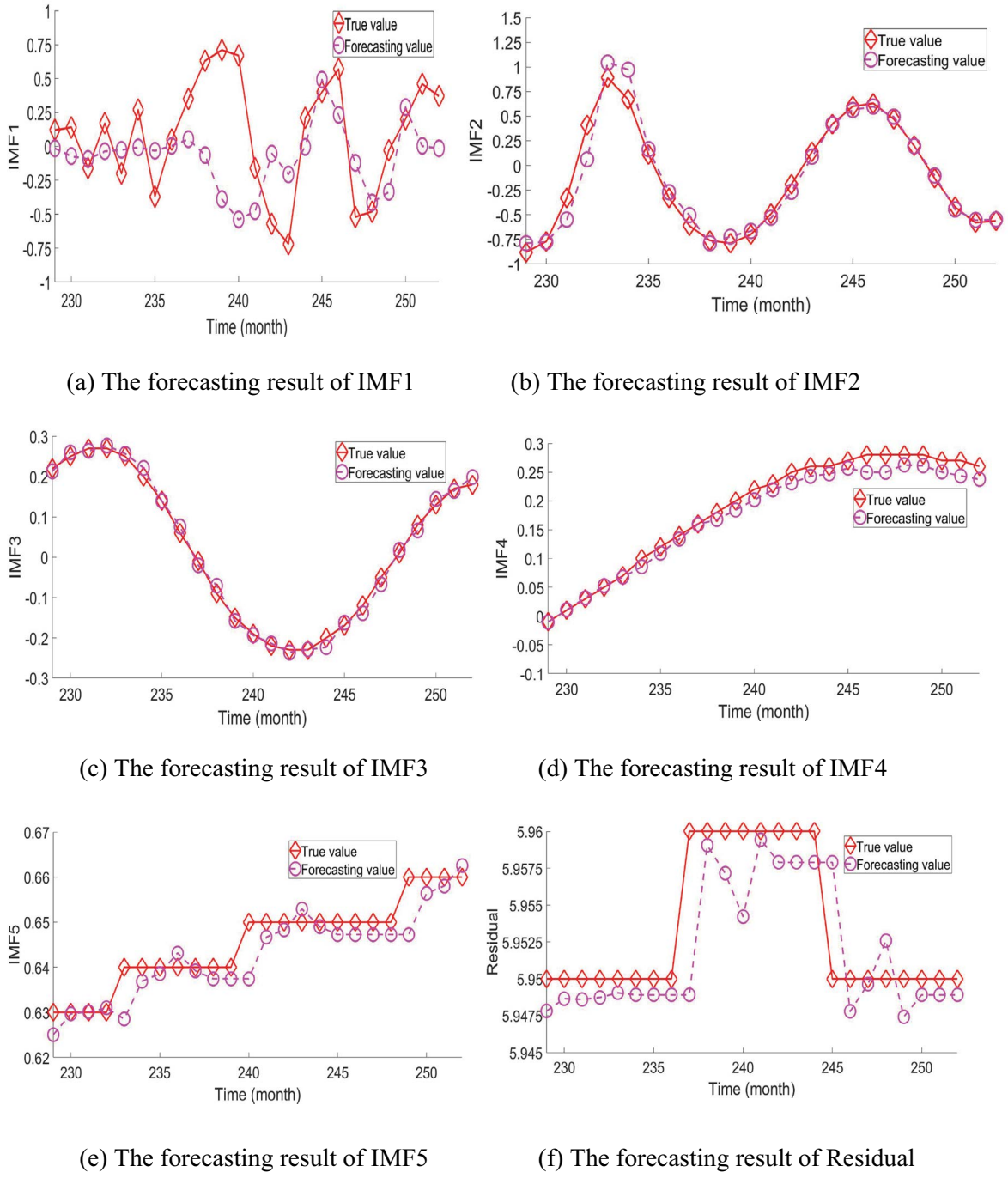

(a) The forecasting result of IMF1

(b) The forecasting result of IMF2

(c) The forecasting result of IMF3

(d) The forecasting result of IMF4

(e) The forecasting result of IMF5

(f) The forecasting result of Residual

Fig. 8. The forecasting result of IMF1-Residual under human over-exploitation.

Table 4
Comparison of forecasting indexes of groundwater depth under two conditions

Human over-exploitation					Normal condition				
True value (*m*)	Forecasting value (*m*)	Absolute error	Relative error (%)	Average relative error (%)	True value (*m*)	Forecasting value (*m*)	Absolute error	Relative error (%)	Average relative error (%)
6.03	5.96	–0.07	1.12		6.03	6.08	0.05	0.84	
6.21	5.99	–0.22	3.59		6.21	6.20	–0.01	0.14	
6.40	6.23	–0.17	2.70		6.4	6.39	–0.01	0.08	
7.49	6.92	–0.57	7.61		6.49	6.54	0.05	0.80	
7.60	7.91	0.31	4.10		6.6	6.66	0.06	0.95	
7.83	7.84	0.01	0.15		6.83	6.72	–0.11	1.59	
6.60	6.96	0.36	5.49		6.6	6.68	0.08	1.21	
6.52	6.52	0.00	0.04		6.52	6.63	0.11	1.74	
6.48	6.27	–0.21	3.18		6.48	6.57	0.09	1.37	
6.56	5.83	–0.73	11.19		6.56	6.61	0.05	0.83	
6.57	5.51	–1.06	16.12		6.57	6.46	–0.11	1.74	
6.59	5.39	–1.20	18.25	5.29	6.59	6.24	–0.35	5.37	1.47
5.96	5.59	–0.37	6.14		5.96	5.96	0.00	0.02	
5.86	6.29	0.43	7.36		5.86	6.04	0.18	3.08	
6.06	6.52	0.46	7.53		6.06	6.17	0.11	1.85	
7.30	7.07	–0.23	3.21		6.3	6.67	0.37	5.87	
7.71	7.76	0.05	0.62		6.71	6.81	0.10	1.47	
7.96	7.55	–0.41	5.18		6.96	7.04	0.08	1.14	
6.78	7.15	0.37	5.45		6.78	6.88	0.10	1.48	
6.62	6.66	0.04	0.60		6.62	6.64	0.02	0.27	
6.80	6.49	–0.31	4.60		6.8	6.65	–0.15	2.28	
6.80	6.82	0.02	0.33		6.8	6.77	–0.03	0.45	
6.92	6.46	–0.46	6.67		6.92	6.89	–0.03	0.38	
6.87	6.48	–0.39	5.73		6.87	6.85	–0.02	0.31	

As can be seen from Table 4, under human over-exploitation, the forecasting effect of the model is worse than normal condition, the average relative error and relative errors are slightly higher than normal condition. This can be considered normal, because under human over-exploitation, the groundwater depth data were disturbed and fluctuated greatly. Furthermore, the variation of groundwater depth itself is a complex process, which is greatly influenced by various uncertain factors, this is bound to influence the forecasting error of the model.

In short, under human over-exploitation, the forecasting accuracy of the model will be slightly reduced, but the relative error is within a reasonable range, the forecasting effect of the EMD-Elman model is still feasible.

5. Conclusions

By forecasting the groundwater depth in the People's Victory Canal Irrigation District, the following conclusions can be drawn.

- Through EMD decomposition, the randomness and non-stationary of groundwater depth series are reduced, which provides a good condition for the forecasting of EMD-Elman coupling model. The relative prediction error of the EMD-Elman coupling model is less than 5.87%, the model has higher accuracy and is better than BPNN model and ENN model. Furthermore, under human over-exploitation, the forecasting accuracy of the EMD-Elman model will be slightly reduced, but the forecasting effect is still feasible. The EMD-Elman model provides a new method for forecasting of groundwater depth.
- EMD decomposition was applied in groundwater depth series, then the ENN was used to forecast the IMF1–residual, which solved the problem that some high-frequency catastrophe data could not be learned well by using the Elman network directly. Compared with the traditional ENN model and BPNN model, the EMD-Elman model can reflect the real change of the groundwater depth series in frequency domain in detail.
- The EMD-Elman coupling model established in this paper also has some reference value to other aspects forecasting. Through EMD decomposition, the complete signal is decomposed into several IMF components and residual, the forecasting value of the complete signal is equal to the sum of the forecasting value of IMF components and the forecasting value of residual. Even though some of IMF components forecasting error are fairly large, however, it is likely that this component is a small part of the signal, even if its forecasting error is large,

it will not have a great impact on the overall forecasting error, when the forecasting values of IMF components and residual are converted into the forecasting value of the complete signal, the forecasting error of the complete signal will weaken.

- Although the forecasting accuracy of the EMD-Elman coupling model is higher, the model also has some shortcomings, such as the artificial setting of network parameters. Furthermore, this paper does only short-term forecasting without long-term forecasting, the forecasting model does not take into account the physical mechanism of groundwater depth change. All these require further research and in depth discussion.

Acknowledgments

This work is financially supported by Collaborative Innovation Center of Water Resources Efficient Utilization and Protection Engineering, Henan Province, Water Environment Governance and Ecological Restoration Academician Workstation of Henan Province, Program for Science & Technology Innovation Talents in Universities of Henan Province (No. 15HASTIT049). Our gratitude is also extended to reviewers for their efforts in reviewing the manuscript and their very encouraging, insightful and constructive comments.

References

[1] Y. Qiao, X.J. Liang, Y.B. Wang, Application and comparison study of two models for groundwater depth prediction, Water Saving Irrig., 3 (2014) 45–53.
[2] N. Zhang, C. Xiao, B. Liu, Groundwater depth predictions by GSM, RBF, and ANFIS models: a comparative assessment, Arab. J. Geosci., 10 (2017) 189.
[3] Y. Choi, Y. Choi, T.H. Le, S. Shin, D. Kwon, Groundwater levels estimation and forecasting by integrating precipitation-based period-dividing algorithm and response surface methodology, Desalin. Water Treat., 54 (2015) 1270–1280.
[4] S. Mohanty, M.K. Jha, S.K. Raul, R.K. Panda, K.P. Sudheer, Using artificial neural network approach for simultaneous forecasting of weekly groundwater levels at multiple sites, Water Resour. Manage., 29 (2015) 5521–5532.
[5] K.A. Mahallawi, J. Mania, A. Hani, Using of neural networks for the prediction of nitrate groundwater contamination in rural and agricultural areas, Environ. Earth Sci., 65 (2012) 917–928.
[6] S. Maiti, R.K. Tiwari, A comparative study of artificial neural networks, Bayesian neural networks and adaptive neuro-fuzzy inference system in groundwater level prediction, Environ. Earth Sci., 71 (2014) 3147–3160.
[7] H.J. Yu, X.H. Wen, Q. Feng, R.C. Deo, J.H. Si, M. Wu, Comparative study of hybrid-wavelet artificial intelligence models for monthly groundwater depth forecasting in extreme arid regions, Northwest China, Water Resour. Manage., 32 (2018) 301–323.
[8] Z.P. Yang, W.X Lu, P. Li, Application of time-series model to predict groundwater regime, J. Hydraul. Eng., 12 (2005) 1475–1479.
[9] B. Sheng, M. Liu, L,M. Huang, Grey self-memory model and its application in the prediction of groundwater depth in Hotan, Xinjiang, J. Northwest A&F Univ. (Nat. Sci. Ed.), 11 (2006) 223–226.
[10] R.F. Li, B. Sheng, J.K. Zhang, Self-memory model for predicting groundwater depth series with periodical fluctuation, Trans. CSAE, 21 (2005) 34–36.
[11] A. Lapedes, R. Farber, Nonlinear Signal Processing Using Neural Networks: Prediction, and System Modelling, LA-VR-87-2662, IEEE International Conference on Neural Networks, Los Alamos, USA, 1987.
[12] N.E. Huang, Z. Shen, S.R. Long, The empirical mode decomposition and the Hilbert spectrum for nonlinear and non-stationary time series analysis, Proc Royal Soc. Lond A, 454 (1998) 903–995.
[13] Y.H. Wang, D.P. Yue, Q. Yu, Dynamic prediction of groundwater depth in Dengkou County based on EMD, J. Northwest Forestry Univ., 32 (2017) 53–59.
[14] S.L. Zhao, Y. Liu, S.Q. Li, Utilizing BP neural network to forecast groundwater regime, J. Agric. Univ. Hebei, 25 (2002) 206–207.
[15] D. Labate, F. La Foresta, G. Occhiuto, Empirical mode decomposition vs. wavelet decomposition for the extraction of respiratory signal from single-channel ECG: a comparison, IEEE Sens. J. 13 (2013).2666–2674.
[16] W.Y. Duan, L.M. Huang, Y. Han, A hybrid EMD-AR model for nonlinear and non-stationary wave forecasting, J. Zhejiang Univ. Sci. A, 17 (2016) 115–127.
[17] C.L. Yeh, H.C. Chang, C.H. Wu, Extraction of single-trial cortical beta oscillatory activities in EEG signals using empirical mode decomposition, Biomed. Eng., 25 (2010) 3–17.
[18] J.L. Elman, Finding structure in time, Cogn. Sci., 14 (1990) 179–211.
[19] P.S. Sastry, G. Santharam, K.P. Unnikrishnan, Memory neuron networks for identification and control of dynamic systems, IEEE Trans. Neural Netw., 5 (1994) 306–319.
[20] C.J. Yu, Y.L. Liu, H.Y. Xiang, M.J. Zhang, Data mining-assisted short-term wind speed forecasting by wavelet packet decomposition and Elman neural network, J. Wind Eng. Ind. Aerodyn., 175 (2018) 136–143.
[21] X.M. Li, T.Y. Zhao, J.L. Zhang, Predication control for indoor temperature time-delay using Elman neural network in variable air volume system, Energy Build., 154 (2017) 545–552.
[22] A.D. Buthina, A. Iftikhar, H. Muhammad, Improving the security in healthcare information system through Elman neural network based classifier, J. Med. Imaging Health Inform., 7 (2017) 1429–1435.
[23] K. Krzysztof, S. Aleksandra, K. Rafal, Multisensor data fusion using Elman neural networks, Appl. Math. Comput., 319 (2018) 236–244.
[24] H. Liu, X.W. Mi, Y.F. Li, Wind speed forecasting method based on deep learning strategy using empirical wavelet transform, long short term memory neural network and Elman neural network, Energy Convers. Manage., 156 (2018) 498–514.